

This article appeared in a journal published by Elsevier. The attached copy is furnished to the author for internal non-commercial research and education use, including for instruction at the authors institution and sharing with colleagues.

Other uses, including reproduction and distribution, or selling or licensing copies, or posting to personal, institutional or third party websites are prohibited.

In most cases authors are permitted to post their version of the article (e.g. in Word or Tex form) to their personal website or institutional repository. Authors requiring further information regarding Elsevier's archiving and manuscript policies are encouraged to visit:

<http://www.elsevier.com/copyright>



Contents lists available at ScienceDirect

Journal of Controlled Release

journal homepage: www.elsevier.com/locate/jconrel

Cationic amphiphilic polyproline helix P11LRR targets intracellular mitochondria

Li Li^{b,1}, Iris Geisler^{b,1}, Jean Chmielewski^{a,b,c}, Ji-Xin Cheng^{a,b,c,*}

^a Weldon School of Biomedical Engineering, Purdue University, West Lafayette, IN 47907, United States

^b Department of Chemistry, Purdue University, West Lafayette, IN 47907, United States

^c Purdue Cancer Center, Purdue University, West Lafayette, IN 47907, United States

ARTICLE INFO

Article history:

Received 2 July 2009

Accepted 9 October 2009

Available online 24 October 2009

Keywords:

Cell penetrating peptide

Mitochondria

ROS

Endocytosis

Membrane translocation

ABSTRACT

We demonstrate that P11LRR, a recently developed amphiphilic polyproline, cell penetrating agent, is able to locate inside the mitochondria of various cell lines when administrated at high concentrations. Mitochondrial targeting was verified by confocal fluorescence co-localization of P11LRR-fluorescein with Mitotracker Red. Elimination of mitochondrial membrane potential dramatically inhibits the localization of P11LRR to mitochondria. Concentration-dependency experiments suggest that cellular internalization of P11LRR occurs via two different pathways: endocytosis and direct transport. Results indicate that the latter pathway predominates at high concentrations of P11LRR, resulting in localization of the agent to the mitochondria. The membrane translocation pathway was further confirmed by two endocytosis inhibitors, cytochalasin D and phenylarsine oxide, and by modulation of plasma membrane potential. The potential of using P11LRR as a mitochondrial drug delivery vector was demonstrated through the delivery of a covalently linked small antioxidant, dimethyltyrosine (Dmt), which allowed for the reduction of chemically induced reactive oxygen species within the mitochondria.

© 2009 Elsevier B.V. All rights reserved.

1. Introduction

The discovery of cell penetrating peptides (CPP) has enabled many advances toward efficient cellular delivery of membrane-impermeable drugs. Attachment of CPPs to hydrophilic macromolecules such as proteins [1–3] or oligonucleotides [4–6] permits cellular uptake of these cell-impermeable molecules. To date, nearly 30 different CPPs have been developed [7], including peptides derived from protein transduction domains such as penetratin [8] and Tat [9], as well as designed and synthesized agents such as transportan [10], oligoarginine [11] and model amphiphilic peptides [12]. The internalization mechanisms of CPPs have been extensively investigated. Based on live cell studies it is generally accepted that endocytosis is the major route [13–15].

The majority of CPPs are cationic in nature, originating from the presence of basic amino acid residues such as arginine and lysine. The cationic property of CPPs is believed to play a crucial role in cellular uptake. Additionally, it has been demonstrated that hydrophobic residues contribute substantially to membrane translocation. For example, it has been shown that stearylation of the Tat peptide

significantly enhanced transfection of DNA into COS-7 cells [16]. In the case of nonpeptidic oligo-guanidinium vectors, placing a tert-butyl-diphenylsilane group (TBDPS) at one terminus of the oligo-guanidinium vectors promoted 4-fold more efficient translocation than the vectors without this hydrophobic moiety [17]. The incorporation of both hydrophilic and hydrophobic amino acids into CPP sequences allows for the creation of overall amphiphilic agents. The role of amphiphilicity in cellular internalization has been examined in various peptide models [18–21]. Generally, the hydrophilic region can serve to concentrate the CPPs near the cell surface through electrostatic interactions with the negatively charged plasma membrane components, while the hydrophobic region can assist membrane destabilization and translocation [22].

P11LRR is such an amphiphilic agent that consists of a pre-organized polyproline scaffolds structure functionalized with cationic and hydrophobic moieties. The polyproline backbone allows for the formation of a polyproline type II helix (PPII) [23]. This type of helix contains three residues per turn with a pitch of 10 Å, thereby aligning every third ring on the same face of the helix. The individual proline monomers comprising the final peptide are first functionalized through O-alkylation of the hydroxyproline monomer to provide the necessary building blocks featuring both hydrophobic and cationic moieties. Specifically, the hydroxyproline monomer was functionalized to yield either a leucine (hydrophobic) or arginine (hydrophilic) mimic through a number of synthetic steps [23]. Such structure grants P11LRR-Fl amphiphilicity with controlled orientation of cationic (blue) and hydrophobic (pink) moieties (Fig. 1). Recent studies have

* Corresponding author. Weldon School of Biomedical Engineering, Purdue University, West Lafayette, IN 47907, United States.

E-mail addresses: chml@purdue.edu (J. Chmielewski), jcheng@purdue.edu (J.-X. Cheng).

¹ These authors contributed equally.

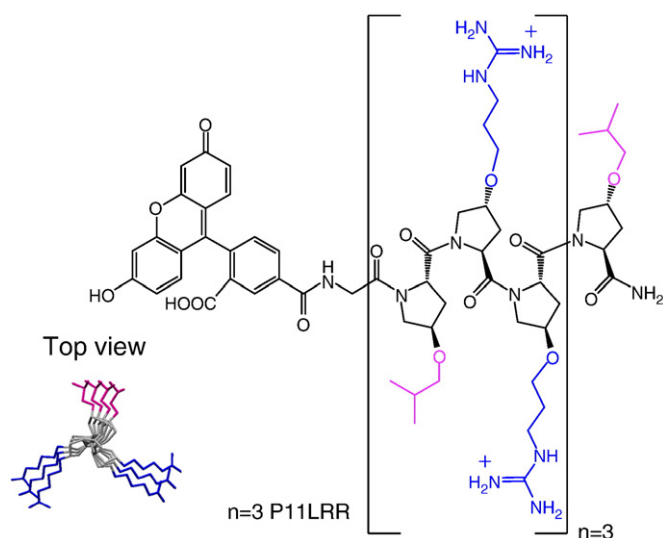


Fig. 1. Macro model and molecular structures of P11LRR-fluorescein (P11LRR-FI). The molecule contains three repeating units. In each unit the hydroxyproline monomer is functionalized to incorporate either a leucine (pink) or arginine (blue) mimic. The modified polyproline oligomers fold into a PPII helix displaying hydrophobic and cationic faces.

shown that P11LRR-FI has greater internalization into cancer cells than the well studied Tat peptide with minimal cytotoxicity [23]. However, the internalization mechanism and subcellular localization of P11LRR-FI was not specifically addressed in this earlier study.

In the present study the internalization mechanism of P11LRR-FI has been carefully investigated. By combining live cell imaging and quantitative flow cytometry analysis, we demonstrate herein that both endocytosis and direct transport are involved in cellular uptake of P11LRR. At relatively low concentrations (e.g., 5.3 μM), endocytosis primarily contributes to cellular uptake of P11LRR, whereas at high concentrations (e.g., 21 μM), direct membrane transport dominates P11LRR internalization. Moreover, the direct transport pathway allows for efficient localization of P11LRR within mitochondria.

2. Materials and methods

2.1. Chemicals

Cell culture medium RPMI 1640, penicillin–streptomycin, Lyso-tracker Red and Mitotracker Red CMXRos were purchased from Invitrogen (Carlsbad, CA). Compactin, cytochalasin D (Cyto-D), carbonylcyanide p-trifluoromethoxy phenyl-hydrazone (FCCP), fetal bovine serum, gramicidin, mevalonate, nigericin, phenylarsine oxide (PAO), and BCA protein assay reagent kit were purchased from Sigma

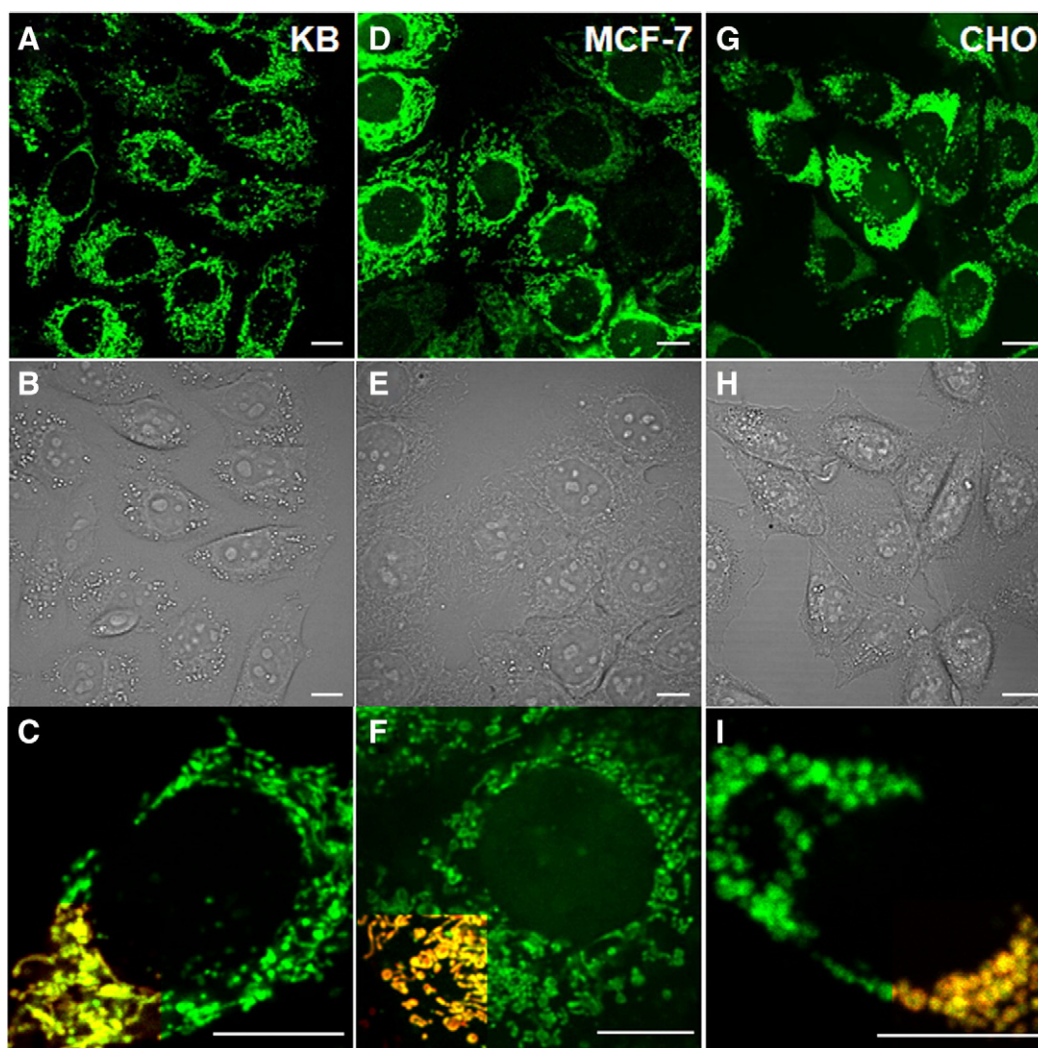


Fig. 2. P11LRR localization into the mitochondria of various cell lines. After incubation with 21 μM P11LRR-FI for 1 h KB cells (A, C), MCF-7 cells (D, F) and CHO cells (G, I), confocal fluorescence imaging showed mitochondrial staining by P11LRR-FI. Corresponding transmission images of multiple cells are shown in (B), (E) and (H). Overlay of P11LRR-FI with Mitotracker Red in (C, F, I) indicates localization of P11LRR-FI in the mitochondria. Bar = 10 μm for all images.

(St. Louis, MO). P11LRR-fluorescein (P11LRR-Fl) and P11LRR-rhodamine (P11LRR-Rh) were synthesized using the same procedure described previously [22]. P11LRR-Dmt was synthesized by adding Fmoc-(S)-2,6-dimethyltyrosine (Dmt) to P11LRR as the final residue in place of a fluorophore using standard solid phase Fmoc chemistry.

2.2. Cell culture

CHO, KB, and MCF-7 cells were maintained in standard or folate-free (for KB cells) RPMI 1640 culture media supplemented with 10% FBS, 100U/mL penicillin, and 0.1 mg/mL streptomycin. The cells were grown in a humidified 5% CO₂ atmosphere at 37 °C. Prior to the imaging experiment, 6 × 10⁴ cells in 1 mL growth medium were seeded on a Petri dish and incubated for 3 to 4 days until confluence.

2.3. Drug treatment

To evaluate the role of mitochondrial or plasma membrane potential in the mitochondrial localization of P11LRR, KB cells were pre-treated with 1 μM FCCP, 1 μM nigericin or 1 μM gramicidin in serum free medium for 30 min and then incubated with P11LRR-Fl in the presence of FCCP, nigericin or gramicidin. Endocytic inhibitors Cyto-D and PAO were used to test the role of endocytosis in P11LRR uptake. KB cells were incubated with 10 μM Cyto-D or 5 μM PAO for 30 min and then with 21 μM P11LRR-

Fl in the presence of Cyto-D or PAO. For all drug treatments, after incubation with P11LRR-Fl the cells were washed three times with PBS and imaged by confocal fluorescence microscopy or analyzed by flow cytometry. All incubations were done in serum free media.

2.4. Laser scanning confocal microscopy

Live cells were imaged on an inverted confocal fluorescence microscope (Olympus, FV1000) equipped with a 60× water immersion objective (Numerical aperture 1.2). Coverslip-bottomed Petri dishes (MatTek, Ashland, MA) were used for high-resolution imaging of cells. A 488-nm Ar⁺ laser was used to excite P11LRR-Fl. A 543-nm HeNe laser was used to excite Mitotracker Red. The typical laser power at the sample was ~80 μW. For co-localization of P11LRR-Fl with Mitotracker Red, cells were incubated at 37 °C with 21 μM (final concentration) P11LRR-Fl for 1 h. Cells were then washed and incubated with 200nM Mitotracker Red (final concentration) for 30 min. Multicolor images were captured by high-speed frame sequential imaging in order to eliminate fluorescence bleed-through.

2.5. Reactive oxygen species (ROS) measurements

MCF-7 breast cancer cells were plated into a 4-well LabTek confocal dish (VWR, NY) at 75,000 cells/well and grown for 2 days at

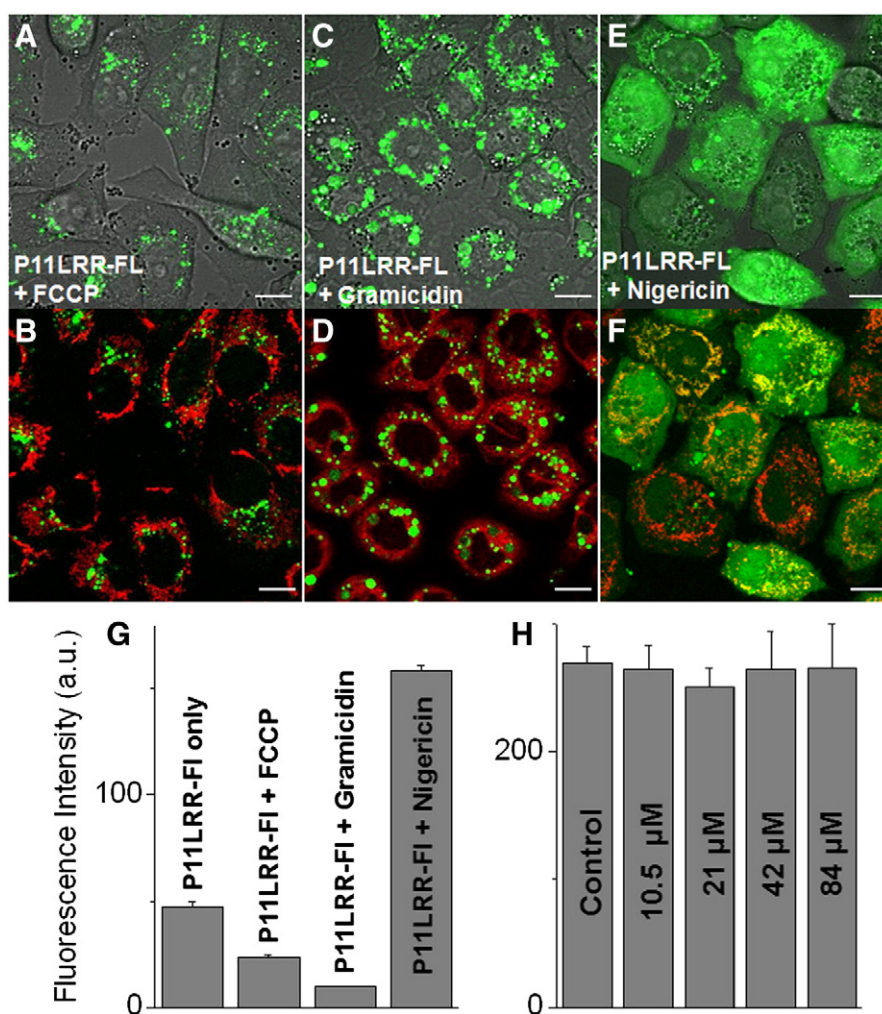


Fig. 3. Cellular uptake and mitochondrial targeting of P11LRR are affected by mitochondrial and plasma membrane potential. Treatment with 1 μM of FCCP (A, B), 1 μM gramicidin (C, D) and 1 μM nigericin (E, F) significantly decreases the localization of P11LRR-Fl in the mitochondria. In the overlay images (B, D, F) the red color represents the signal of Mitotracker Red. Bar = 10 μm. (G) Flow cytometry quantification of P11LRR-Fl uptake in normal cells, FCCP, gramicidin and nigericin treated cells. (H) Effects of various concentrations of unlabeled P11LRR on the mitochondrial membrane potential as determined by flow cytometry. The standard deviations were obtained from three independent measurements.

37 °C and 5% CO₂ in RPMI 1640 media supplemented with 10% HIFBS. After 2 days the media was removed and the cells were treated with either fresh media or incubated with 40 μM P11LRR-Dmt for 2.5 h in serum free RPMI 1640. After incubation, the cells were washed 3× with PBS and incubated for an additional 2 h with 500 μM t-BHP (Aldrich, WI) in serum free RPMI 1640. t-BHP was removed after 2 h and the cells were washed 3× with PBS and labeled with 20 μM of the ROS indicator carboxy H₂-DCFDA (C-400, Invitrogen, CA) for 30 min in PBS. After 30 min the cells were washed 3× with PBS and allowed to recover for 30 min in fresh media at 37 °C and 5% CO₂ before confocal microscope imaging. A 488 nm laser was used for excitation (see above). All images were obtained at equal laser intensity to allow for direct comparison.

2.6. Flow cytometry

Cellular uptake of P11LRR-FI was quantified by flow cytometry. The KB cells were seeded into 12-well plates at a density of 0.5×10^5 cells/well in 1 mL of media and grown in a humidified 5% CO₂ atmosphere at 37 °C for 3 days. Cells were incubated for 1 h in 1 mL media with P11LRR-FI at indicated concentrations. Following the incubation, the cells were washed three times with PBS, gently dissociated from the wells with 100 μL of cell dissociation solution, and then re-suspended in 300 μL of culture medium. Cellular fluorescence was measured on a flow cytometer (BD FACSCalibur™) with 488 nm excitation. Control cells that were not treated with the agents were also analyzed to determine the background fluorescence level.

3. Results and discussion

Intracellular localization of P11LRR was studied by confocal fluorescence imaging of P11LRR-FI in live cells. After incubation with 21 μM P11LRR-FI at 37 °C for 1 h, elongated and thread-like organelles labeled by the fluorescent peptide were observed in the cytoplasm of majority of KB cells (Fig. 2A). The morphology of the organelles was observed to be unlike cytosolic vesicles, but more closely resembled mitochondria. In order to confirm that P11LRR was localized to mitochondria, a co-localization study of P11LRR-FI with Mitotracker Red (a mitochondria-specific dye) was performed. The confocal fluorescence images in Fig. 2C clearly demonstrated a high level of co-localization of P11LRR-FI with Mitotracker Red in KB cells, corroborating the association of P11LRR with mitochondria. This phenomenon was also observed in other cell types such as MCF-7 and CHO cells, as shown in Fig. 2D–F and G–I, respectively. No perturbation of cell morphology was found (Fig. 2B, E and H). The same phenomenon was observed at 50 μM P11LRR (data not shown). These results suggest that P11LRR is capable of targeting mitochondria of different cell types. In order to rule out the possibility of mitochondrial targeting due to the effect of conjugated dye, we additionally tested rhodamine labeled P11LRR (P11LRR-Rh), which also indicated mitochondrial localization (Fig. S1).

One of the major roles of mitochondria in cellular metabolism is the synthesis of ATP by oxidative phosphorylation via the respiratory chain. This process creates a transmembrane electrochemical gradient, which includes contributions from both a membrane potential and a pH difference [24]. Therefore, lipophilic cations such as triphenylphosphonium cations (TPP) and rhodamine 123 can target the mitochondrial inner membrane and accumulate in the matrix in accordance to the negative mitochondrial transmembrane potential [25–27]. In order to determine whether the mitochondrial transmembrane potential also directs the localization of P11LRR to mitochondria, we treated KB cells with FCCP, a selective decoupler of mitochondrial membrane potential. KB cells were pre-incubated for 60 min with media containing 1 μM FCCP to depolarize mitochondria [28]. Subsequent confocal fluorescence imaging showed little co-localization of P11LRR-FI with Mitotracker Red in FCCP treated cells (Fig. 3A–B), indicating a critical role of mito-

chondrial transmembrane potential in attracting P11LRR to mitochondria. FCCP also decreased the cellular uptake of P11LRR-FI by 50% as quantified by flow cytometry (Fig. 3G).

The integrity of ATP levels was also investigated to determine if P11LRR would manipulate mitochondrial function. To this end, MCF-7 cells were incubated with various concentrations of unlabeled P11LRR for 5 h followed by the determination of ATP levels using an ApoSENSOR Assay Kit (Fig. S4). The data obtained indicated that P11LRR has no significant effect on the overall ATP level of the cell. Therefore, P11LRR does not seem to negatively effect mitochondrial function. Tat was used as a negative control, as it was not expected to have an effect on ATP levels.

The mitochondrial targeting behavior of P11LRR is consistent with its structural properties: P11LRR features a rigid polyproline scaffold with a pre-organized structure to systematically position cationic and hydrophobic moieties. The guanidinium groups positioned along the polyproline backbone allow for the display of six positive charges within the peptide. Conceivably, these charges facilitate the movement of P11LRR to mitochondria in response to the highly negative mitochondrial transmembrane potential as shown above. Previously reported mitochondrial targeting peptides are also rich in positive charged residues [29–31]. The mitochondrial outer membrane is known to be permeable to ions and solutes smaller than 6 kDa [32], which would allow P11LRR-FI (MW = 2384) to efficiently penetrate into the intermembrane space. The hydrophobic face of P11LRR may facilitate the insertion of the peptide into the mitochondrial inner

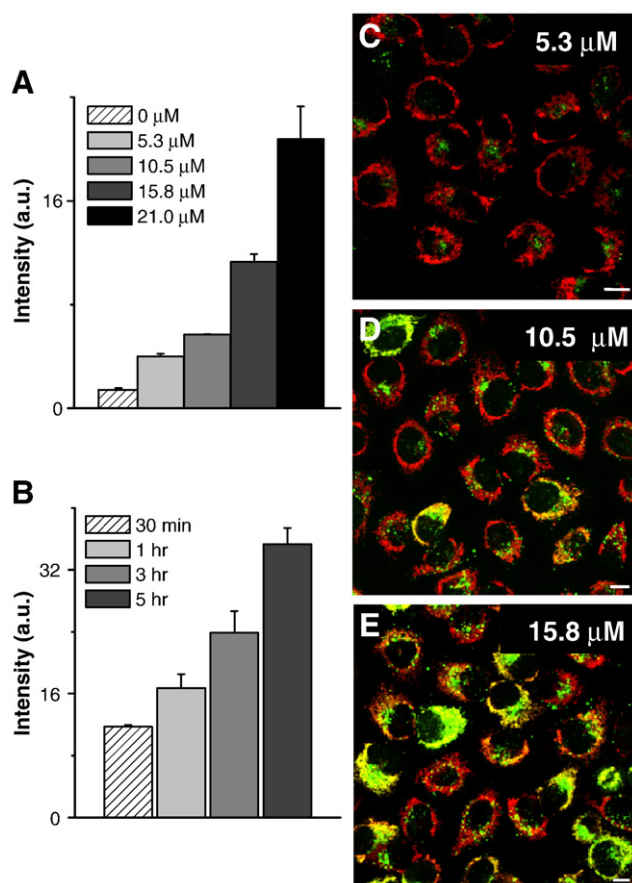


Fig. 4. Concentration-dependent uptake of P11LRR-FI. (A) Flow cytometry analysis of internalized P11LRR-FI (various concentrations) in KB cells after incubation for one hour at 37 °C. (B) Flow cytometry analysis of internalized P11LRR-FI in KB cells after incubation with 21 μM P11LRR-FI for different periods of time. Confocal images show the distribution of P11LRR-FI in KB cells after incubating KB cells with 5.3 μM (C) 10.5 μM (D) and 15.8 μM (E) P11LRR-FI for one hour at 37 °C. In (C–E) the red signal represents Mitotracker Red.

membrane. As supporting evidence for the strong association of P11LRR with mitochondria, we observed that P11LRR-FI remained associated with mitochondria after 48 h incubation with fresh media (Fig. S2).

To test whether the uptake of P11LRR into mitochondria could alter the mitochondrial membrane potential, Mitotracker Red (a potential sensitive dye) was used as an indicator of mitochondrial membrane potential change in P11LRR treated KB cells. In this experiment KB cells were pre-treated with unlabeled P11LRR at different concentrations for 5 h, followed by incubation with Mitotracker Red for 30 min in the presence of unlabeled P11LRR. The intracellular intensities of Mitotracker Red were measured by flow cytometry. The results (Fig. 3H) show that P11LRR does not have a significant impact on the mitochondrial membrane potential even at a concentration of 84 μM .

In order for P11LRR to associate with mitochondria, P11LRR should be able to diffuse inside of the cytoplasm. Two possible pathways exist that would allow for the internalization of P11LRR into the cytoplasm. One being the release of P11LRR from endosomes into the cytosol after internalization via endocytosis and followed by the peptides migration to mitochondria [33]. Another pathway is the direct translocation of P11LRR across the plasma membrane and its diffusion to mitochondria in response to the mitochondrial membrane potential. The direct transport mechanism has been observed in the uptake of some cell penetrating peptides including Tat [34]. Horton et al. have recently demonstrated that a group of mitochondrial penetrating peptides are able to permeate the plasma membrane in a potential-driven manner [29]. To determine whether a direct transport mechanism exists to assist the targeting of P11LRR to mitochondria, we modulated the plasma membrane potential with two different agents. When KB cells were treated with gramicidin, an agent that is known to depolarize the plasma membrane [35], P11LRR-FI is no longer observed within the mitochondria, with remaining punctuate fluorescence suggesting localization within cytosolic vesicles other than mitochondria (Fig. 3C, D). Accordingly, the flow cytometry results showed 80% decrease of P11LRR-FI uptake (Fig. 3G). However, when KB cells were

treated with nigericin, a drug that can induce plasma membrane hyperpolarization [36], a more diffuse signal for P11LRR-FI was observed inside of the cytoplasm. The treatment with nigericin also resulted in a 3.3-fold increase in P11LRR-FI uptake (Fig. 3G). The dependence of P11LRR uptake on the plasma membrane potential supports the existence of a direct transport pathway.

In order to further gain insight into the cellular internalization mechanism of P11LRR-FI, we have utilized flow cytometry to quantify P11LRR-FI accumulation inside cells at different concentrations of administered peptide. The results showed that cellular uptake of P11LRR-FI was concentration-dependent and non-saturable (Fig. 4A). A nonlinear increase of uptake was observed with increasing P11LRR-FI concentration. It is important to note that P11LRR-FI uptake was dramatically enhanced when the concentrations were above 10.5 μM . Confocal studies indicated that P11LRR-FI mainly localized in cytoplasmic vesicles, such as endosomes, at concentrations as low as 5.25 μM , with no co-localization with Mitotracker Red (Fig. 4C). At increased concentrations of 10.5 and 15.8 μM , more cells exhibited localization of P11LRR-FI to the mitochondria, *i.e.*, the merged images in Fig. 4D and E showed an increased overlap between P11LRR-FI (green) and Mitotracker Red (red). A kinetic analysis of the internalization process of P11LRR-FI at 21 μM showed progressively increasing internalization with time, without reaching saturation after 5 h incubation (Fig. 4B), indicative of a direct transport mechanism.

The above concentration-dependent uptake study suggests that both endocytosis and direct transport are involved in cellular uptake of P11LRR. At relatively low concentration (*e.g.* 5.3 μM), endocytosis makes a major contribution to the cellular uptake of P11LRR (Fig. 4C). Interestingly, Pooga et al. recently demonstrated that CPPs are able to cause the formation of three different endo-lysosomal vesicles, guided by CPP characteristics, concentration and time. Efflux of CPP-cargo complex is believed to occur, depending on time, CPP characteristics and the pH of the vesicle formed [37]. In case of P11LRR, a majority of the peptide remained in endosomes even after an 8 h incubation (Fig. S3), therefore we believe that mitochondrial staining by P11LRR-FI is unlikely due to endosomal escape.

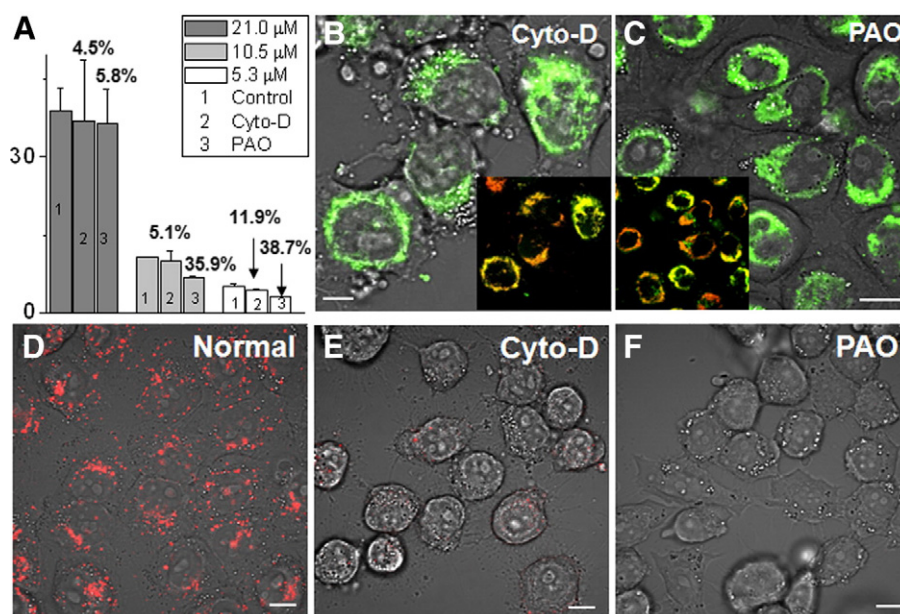


Fig. 5. P11LRR-FI is able to directly translocate across the plasma membrane. (A) FACS data showing that Cyto-D and PAO treatment has a greater impact on the uptake of P11LRR-FI at low concentrations. The decrease of uptake in the presence of inhibitors as compared to normal cells is expressed in percentages. Both Cyto-D (B) and PAO (C) treatment does not block the localization of P11LRR-FI to mitochondria at a concentration of 21 μM P11LRR-FI. Both inhibitor treated cells internalizing P11LRR-FI are co-localized with Mitotracker Red as shown in the overlay images placed in the corners of (B) and (C). D–F represent control experiments showing inhibition of endocytosis by Cyto-D and PAO. Confocal fluorescence images of DiIC18 uptake in normal KB cells, Cyto-D treated and PAO treated KB cells are shown in (D), (E), and (F), respectively. KB cells in (D) were treated with 200 nM DiIC18 for 15 min at 0 $^{\circ}\text{C}$, rinsed three times with PBS and then placed back into the incubator for 1 h. KB cells in (E) and (F) were pre-treated with 10 μM Cyto-D or 5 μM PAO for 30 min at 37 $^{\circ}\text{C}$, then treated with 200 nM DiIC18 in the presence of the endocytotic inhibitors. Bar = 10 μm .

In contrast, at high concentrations (e.g. 21 μM) direct membrane transport may dominate the P11LRR internalization, resulting in effective localization of P11LRR-FI in mitochondria as shown in Fig. 2. Known inhibitors of endocytosis, cytochalasin D (Cyto-D) and phenylarsine oxide (PAO), were used to further examine the role of endocytosis for P11LRR-FI administered at different concentrations. KB cells were treated with 10 μM Cyto-D which inhibits endocytosis by disrupting the actin cytoskeleton [38], or 5 μM PAO, a general endocytosis inhibitor [39,40]. Quantitative flow cytometry analysis demonstrated that cell treatment with Cyto-D and PAO lead to decreased uptake of P11LRR-FI at lower concentrations (Fig. 5A). These data support the coexistence of endocytosis and direct transport for P11LRR uptake as stated above. In accordance with previously obtained flow cytometry data, the overlaid (P11LRR-FI and Mito-tracker Red) confocal images shown in Fig. 5B and C demonstrate that neither Cyto-D nor PAO treatment was able to block localization of P11LRR-FI to mitochondria at a concentration of 21 μM . In a control experiment the ability of Cyto-D and PAO to block endocytosis of DiIC18 was confirmed by a significant decrease of DiIC18 internalization into KB cells as shown in Fig. 5D–F.

Accumulated evidence has shown that mitochondrial damage leads to cardiovascular disease, diabetes, and various neurodegenerative diseases such as Parkinson's and Alzheimer's diseases [41]. Mutations in mitochondrial DNA are also associated with a wide range of human diseases such as Friedreich's ataxia and Wilson's disease [42,43]. Currently the most often reported mitochondrial delivery carriers are delocalized lipophilic cations such as TPP cation and rhodamine 123 [25,44]. Delivery of non-polar molecules such as antioxidants [45] and peptide nucleic acids (PNA) oligomers [46] using TPP has been reported. Cell permeable Szeto–Schiller peptide antioxidants that target the mitochondria inner membrane represent another approach to delivering antioxidants to mitochondria [47].

The mitochondria-targeting property of P11LRR opens new opportunities for a CPP to serve as a novel mitochondrial drug delivery vector. To demonstrate the use of a CPP for the delivery of small functional molecules into the mitochondria the P11LRR derivative P11LRR-Dmt (see Fig. 6A) was constructed. Specifically, the (S)-2,6-dimethyltyrosine (Dmt) residue has previously been shown to be an effective scavenger of reactive oxygen species (ROS) [48]. Therefore, the delivery of Dmt covalently linked to P11LRR has been chosen to

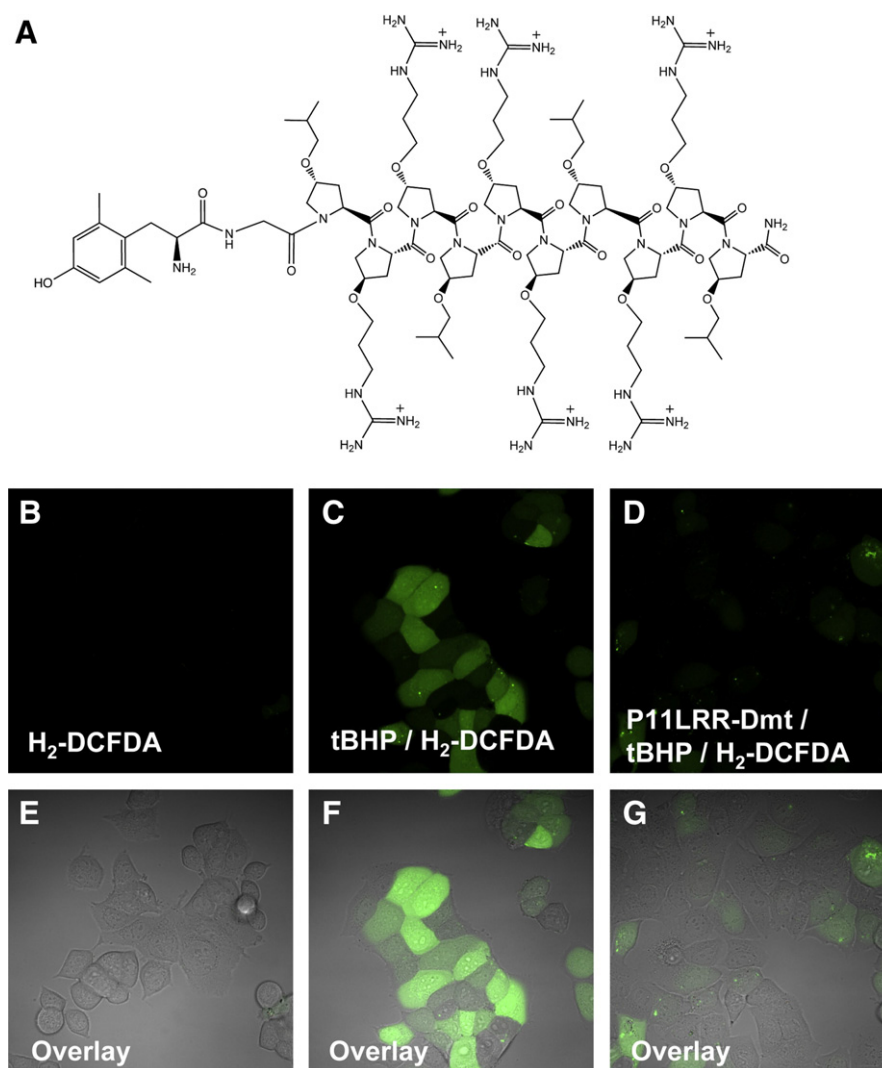


Fig. 6. P11LRR-Dmt treatment leads to a decrease in ROS. (A) Chemical structure of P11LRR-Dmt. (B–G) Detection of ROS in cells treated with and without P11LRR-Dmt (40 μM , 2.5 h) using carboxy H₂-DCFDA (20 μM , 30 min) for visualization of ROS generated (green channel and transmission/green channel overlays). (B) Cells treated with H₂-DCFDA only (green channel) (C) Transmission image overlaid with green channel of B. (D) Production of ROS was induced using t-butyl hydroperoxide (t-BHP) (500 μM , 2 h), ROS production visualized using H₂-DCFDA (green channel). (E) Transmission image overlaid with green channel of D. (F) Cells pre-treated with P11LRR (40 μM , 2.5 h), followed by treatment with t-BHP and H₂-DCFDA as above (green channel). (G) Transmission image overlaid with green channel of F.

investigate the potential of P11LRR as a functional mitochondrial delivery system. The generation of ROS inside cells can be achieved using tert-butyl hydroperoxide (t-BHP), an agent known to lead to increased ROS production in mitochondria [49]. Specifically, cells were pre-treated with and without P11LRR-Dmt (40 μ M, 2.5 h) before an additional incubation of cells with t-BHP (500 μ M, 2 h). The degree of ROS production was visualized using confocal microscopy, after treatment with H₂-DCFDA (20 μ M), an oxidation sensitive non-fluorescent probe that becomes fluorescent upon oxidation by ROS [50,51]. There was no evidence of ROS in untreated cells (Fig. 6B, C), whereas treatment of cells with t-BHP led to a noticeable increase in ROS (Fig. 6D, E). Pre-incubation of cells with P11LRR-Dmt, followed by t-BHP treatment led to an overall decrease of ROS generated (Fig. 6F, G), which suggests a successful delivery of P11LRR-Dmt to the mitochondria. These data further corroborate the mitochondrial localization of P11LRR and its potential use as a mitochondrial delivery agent.

4. Conclusions

The work presented herein demonstrates that a polyproline agent, P11LRR, can target mitochondria of various cell types. After incubation of KB, CHO, and MCF-7 cells with P11LRR at concentrations of 21 μ M or above, P11LRR was efficiently localized in the mitochondria, verified by co-localization of P11LRR-Fl with Mitotracker Red and P11LRR-Rh with Mitotracker Green. The accumulation of P11LRR-Fl in mitochondria was found to be driven by the mitochondrial transmembrane potential, and cellular uptake of P11LRR-Fl depended on plasma membrane potential. Concentration-dependent experiments suggest that the cellular internalization of P11LRR-Fl may involve both endocytosis and direct transport pathways. At high concentrations the direct transport pathway dominates and accounts for the extensive mitochondrial localization. Increasing plasma membrane permeability through metabolic depletion of cholesterol increased the uptake of P11LRR-Fl and also resulted in greater accumulation of P11LRR-Fl to mitochondria. The potential of P11LRR as a mitochondrial delivery agent was also demonstrated through the delivery of a covalently linked small antioxidant, which allowed for the reduction of ROS inside MCF-7 breast cancer cells. Taken together, these results suggest the exciting possibility of using P11LRR as a new type of mitochondrial drug delivery vector for various cargoes.

Acknowledgements

This work was partly supported by NSF grant 0416785-MCB to J. Cheng.

Appendix A. Supplementary data

Supplementary data associated with this article can be found, in the online version, at doi:10.1016/j.jconrel.2009.10.012.

References

- [1] M. Peitz, K. Pfannkuche, K. Rajewsky, F. Edenhofer, Ability of the hydrophobic FGF and basic TAT peptides to promote cellular uptake of recombinant Cre recombinase: a tool for efficient genetic engineering of mammalian genomes, *Proc. Natl. Acad. Sci. U. S. A.* 99 (7) (2002) 4489–4494.
- [2] M. Silhol, M. Tyagi, M. Giacca, B. Lebleu, E. Vives, Different mechanisms for cellular internalization of the HIV-1 Tat-derived cell penetrating peptide and recombinant proteins fused to Tat, *Eur. J. Biochem.* 269 (2) (2002) 494–501.
- [3] M. Pooga, C. Kut, M. Kihlmark, M. Hallbrink, S. Farnaes, R. Raid, T. Land, E. Hallberg, T. Bartfai, U.L.O. Langel, Cellular translocation of proteins by transportan, *FASEB J.* 15 (8) (2001) 1451–1453.
- [4] J.J. Turner, A.A. Arzumanov, M.J. Gait, Synthesis, cellular uptake and HIV-1 Tat-dependent trans-activation inhibition activity of oligonucleotide analogues disulfide-conjugated to cell-penetrating peptides, *Nucleic Acids Res.* 33 (1) (2005) 27–42.
- [5] A. Astriab-Fisher, D. Sergueev, M. Fisher, B.R. Shaw, R.L. Juliano, Conjugates of antisense oligonucleotides with the Tat and antennapedia cell-penetrating peptides: effects on cellular uptake, binding to target sequences, and biologic actions, *Pharm. Res.* V19 (6) (2002) 744–754.
- [6] M.J. Gait, Peptide-mediated cellular delivery of antisense oligonucleotides and their analogues, *Cell. Mol. Life Sci.* V60 (5) (2003) 844–853.
- [7] R. Fischer, M. Fotin-Mleczek, H. Hufnagel, R. Brock, Break on through to the other side – biophysics and cell biology shed light on cell-penetrating peptides, *ChemBioChem* 6 (12) (2005) 2126–2142.
- [8] D. Derossi, A.H. Joliet, G. Chassaing, A. Prochiantz, The third helix of the Antennapedia homeodomain translocates through biological membranes, *J. Biol. Chem.* 269 (14) (1994) 10444–10450.
- [9] E. Vives, P. Brodin, B. Lebleu, A truncated HIV-1 tat protein basic domain rapidly translocates through the plasma membrane and accumulates in the cell nucleus, *J. Biol. Chem.* 272 (25) (1997) 16010–16017.
- [10] U. Soomets, M. Lindgren, X. Gallet, M. Hallbrink, A. Elmquist, L. Balaspiri, M. Zorko, M. Pooga, R. Brasseur, U. Langel, Deletion analogues of transportan, *Biochim. Biophys. Acta* 1467 (1) (2000) 165–176.
- [11] S. Futaki, T. Suzuki, W. Ohashi, T. Yagami, S. Tanaka, K. Ueda, Y. Sugiura, Arginine-rich peptides. An abundant source of membrane-permeable peptides having potentials as carriers for intracellular protein delivery, *J. Biol. Chem.* 276 (8) (2001) 5836–5840.
- [12] J. Oehlke, A. Scheller, B. Wiesner, E. Krause, M. Beyermann, E. Klauschen, M. Melzig, M. Bienert, Cellular uptake of an [alpha]-helical amphipathic model peptide with the potential to deliver polar compounds into the cell interior non-endocytically, *Biochim. Biophys. Acta* 1414 (1–2) (1998) 127–139.
- [13] J.S. Wadia, S.F. Dowdy, Transmembrane delivery of protein and peptide drugs by TAT-mediated transduction in the treatment of cancer, *Adv. Drug Deliv. Rev.* 57 (4) (2005) 579–596.
- [14] H. Brooks, B. Lebleu, E. Vives, Tat peptide-mediated cellular delivery: back to basics, *Adv. Drug Deliv. Rev.* 57 (4) (2005) 559–577.
- [15] E. Vives, Present and future of cell-penetrating peptide mediated delivery systems: “is the Trojan horse too wild to go only to Troy?”, *J. Control. Release* 109 (1–3) (2005) 77–85.
- [16] I.A. Khalil, S. Futaki, M. Niwa, Y. Baba, N. Kaji, H. Kamiya, H. Harashima, Mechanism of improved gene transfer by the N-terminal stearylation of octarginine: enhanced cellular association by hydrophobic core formation, *Gene Ther.* 11 (7) (2004) 636–644.
- [17] J. Fernández-Carneado, M. VanGool, V. Martos, S. Castel, P. Prados, J. deMendoza, E. Giralt, Highly efficient, nonpeptidic oligoguanidinium vectors that selectively internalize into mitochondria, *J. Am. Chem. Soc.* 127 (3) (2005) 869–874.
- [18] M.C. Morris, J. Depollier, J. Mery, F. Heitz, G. Divita, A peptide carrier for the delivery of biologically active proteins into mammalian cells, *Nat. Biotechnol.* 19 (12) (2001) 1173–1176.
- [19] K. Rittner, A. Benavente, A. Bompard-Sorlet, F. Heitz, G. Divita, R. Brasseur, E. Jacobs, New basic membrane-destabilizing peptides for plasmid-based gene delivery in vitro and in vivo, *Molec. Ther.* 5 (2) (2002) 104–114.
- [20] L. Crespo, G. Sanclimens, B. Montaner, R. Perez-Tomas, M. Royo, M. Pons, F. Albericio, E. Giralt, Peptide dendrimers based on polyproline helices, *J. Am. Chem. Soc.* 124 (30) (2002) 8876–8883.
- [21] J. Farrera-Sinfreu, E. Giralt, S. Castel, F. Albericio, M. Royo, Cell-penetrating cis- γ -amino-L-proline-derived peptides, *J. Am. Chem. Soc.* 127 (26) (2005) 9459–9468.
- [22] J. Fernández-Carneado, M.J. Kogan, S. Pujals, E. Giralt, Amphipathic peptides and drug delivery, *Pept. Sci.* 76 (2) (2004) 196–203.
- [23] Y.A. Fillon, J.P. Anderson, J. Chmielewski, Cell penetrating agents based on a polyproline helix scaffold, *J. Am. Chem. Soc.* 127 (33) (2005) 11798–11803.
- [24] R.A.J. Smith, C.M. Porteous, A.M. Gane, M.P. Murphy, Delivery of bioactive molecules to mitochondria in vivo, *Proc. Natl. Acad. Sci. U. S. A.* 100 (9) (2003) 5407–5412.
- [25] S.-S. Sheu, D. Nauduri, M.W. Anders, Targeting antioxidants to mitochondria: a new therapeutic direction, *Biochim. Biophys. Acta* 1762 (2) (2006) 256–265.
- [26] R.C. Scaduto Jr., L.W. Grotyohann, Measurement of mitochondrial membrane potential using fluorescent rhodamine derivatives, *Biophys. J.* 76 (1) (1999) 469–477.
- [27] G. Solaini, G. Sgarbi, G. Lenaz, A. Baracca, Evaluating mitochondrial membrane potential in cells, *Biosci. Rep.* 27 (1) (2007) 11–21.
- [28] M.F. Ross, T.D. Ros, F.H. Blaikie, T.A. Prime, C.M. Porteous, I.I. Severina, V.P. Skulachev, H.G. Kjaergaard, R.A.J. Smith, M.P. Murphy, Accumulation of lipophilic dicationic by mitochondria and cells, *Biochem. J.* 400 (2006) 199–208.
- [29] K.L. Horton, K.M. Stewart, S.B. Fonseca, Q. Guo, S.O. Kelley, Mitochondria-penetrating peptides, *Chem. Biol.* 15 (4) (2008) 375–382.
- [30] K. Zhao, G. Luo, S. Giannelli, H.H. Szeto, Mitochondria-targeted peptide prevents mitochondrial depolarization and apoptosis induced by tert-butyl hydroperoxide in neuronal cell lines, *Biochem. Pharmacol.* 70 (12) (2005) 1796–1806.
- [31] K. Zhao, G.-M. Zhao, D. Wu, Y. Soong, A.V. Birk, P.W. Schiller, H.H. Szeto, Cell-permeable peptide antioxidants targeted to inner mitochondrial membrane inhibit mitochondrial swelling, oxidative cell death, and reperfusion injury, *J. Biol. Chem.* 279 (33) (2004) 34682–34690.
- [32] K.B. Wallace, A.A. Starkov, Mitochondrial targets of drug toxicity, *Annu. Rev. Pharmacol. Toxicol.* 40 (1) (2000) 353–388.
- [33] M. Magzoub, A. Pramanik, A. Graslund, Modeling the endosomal escape of cell-penetrating peptides: transmembrane pH gradient driven translocation across phospholipid bilayers, *Biochemistry* 44 (45) (2005) 14890–14897.
- [34] F. Duchardt, M. Fotin-Mleczek, H. Schwarz, R. Fischer, R. Brock, A comprehensive model for the cellular uptake of cationic cell-penetrating peptides, *Traffic* 8 (7) (2007) 848–866.
- [35] F. Di Virgilio, P.D. Lew, T. Andersson, T. Pozzan, Plasma membrane potential modulates chemotactic peptide-stimulated cytosolic free Ca²⁺ changes in human neutrophils, *J. Biol. Chem.* 262 (10) (1987) 4574–4579.
- [36] S. Davis, M.J. Weiss, J.R. Wong, T.J. Lampidis, L.B. Chen, Mitochondrial and plasma membrane potentials cause unusual accumulation and retention of rhodamine 123 by human breast adenocarcinoma-derived MCF-7 cells, *J. Biol. Chem.* 260 (25) (1985) 13844–13850.

- [37] H. Raagel, P. Saalik, M. Hansen, U. Langel, M. Pooga, CPP-protein constructs induce a population of non-acidic vesicles during trafficking through endo-lysosomal pathway, *J. Control. Release* 139 (2) (2009) 108–117.
- [38] S.L. Brenner, E.D. Korn, Substoichiometric concentrations of cytochalasin D inhibit actin polymerization. Additional evidence for an F-actin treadmill, *J. Biol. Chem.* 254 (20) (1979) 9982–9985.
- [39] A.E. Gibson, R.J. Noel, J.T. Herlihy, W.F. Ward, Phenylarsine oxide inhibition of endocytosis: effects on asialofetuin internalization, *Am. J. Physiol., Cell Physiol.* 257 (2) (1989) C182–184.
- [40] S.C. Frost, M.D. Lane, E.M. Gibbs, Effect of phenylarsine oxide on fluid phase endocytosis: further evidence for activation of the glucose transporter, *J. Cell. Physiol.* 141 (3) (1989) 467–474.
- [41] K. Hirai, G. Aliev, A. Nunomura, H. Fujioka, R.L. Russell, C.S. Atwood, A.B. Johnson, Y. Kress, H.V. Vinters, M. Tabaton, S. Shimohama, A.D. Cash, S.L. Siedlak, P.L.R. Harris, P.K. Jones, R.B. Petersen, G. Perry, M.A. Smith, Mitochondrial abnormalities in Alzheimer's disease, *J. Neurosci.* 21 (9) (2001) 3017–3023.
- [42] D.C. Wallace, Mitochondrial diseases in man and mouse, *Science* 283 (5407) (1999) 1482–1488.
- [43] T. Pulkes, M.G. Hanna, Human mitochondrial DNA diseases, *Adv. Drug Deliv. Rev.* 49 (1–2) (2001) 27–43.
- [44] J.S. Armstrong, Mitochondrial medicine: pharmacological targeting of mitochondria in disease, *Br. J. Pharmacol.* 151 (8) (2007) 1154–1165.
- [45] R.A.J. Smith, C.M. Porteous, C.V. Coulter, M.P. Murphy, Selective targeting of an antioxidant to mitochondria, *Eur. J. Biochem.* 263 (3) (1999) 709–716.
- [46] A. Muratovska, R.N. Lightowers, R.W. Taylor, D.M. Turnbull, R.A.J. Smith, J.A. Wilce, S.W. Martin, M.P. Murphy, Targeting peptide nucleic acid (PNA) oligomers to mitochondria within cells by conjugation to lipophilic cations: implications for mitochondrial DNA replication, expression and disease, *Nucleic Acids Res.* 29 (9) (2001) 1852–1863.
- [47] H.H. Szeto, P.W. Schiller, K. Zhao, G. Luo, Fluorescent dyes alter intracellular targeting and function of cell-penetrating tetrapeptides, *FASEB J.* 19 (1) (2005) 118–120.
- [48] H.H. Szeto, Cell-permeable, mitochondrial-targeted, peptide antioxidants, *AAPS J.* 8 (2) (2006) E277–283.
- [49] K. Zhao, G.M. Zhao, D. Wu, Y. Soong, A.V. Birk, P.W. Schiller, H.H. Szeto, Cell-permeable peptide antioxidants targeted to inner mitochondrial membrane inhibit mitochondrial swelling, oxidative cell death, and reperfusion injury, *J. Biol. Chem.* 279 (33) (2004) 34682–34690.
- [50] A.M. Miles, D.S. Bohle, P.A. Glassbrenner, B. Hansert, D.A. Wink, M.B. Grisham, Modulation of superoxide-dependent oxidation and hydroxylation reactions by nitric oxide, *J. Biol. Chem.* 271 (1) (1996) 40–47.
- [51] J.A. Royall, H. Ischiropoulos, Evaluation of 2', 7'-dichlorofluorescein and dihydrorhodamine 123 as fluorescent probes for intracellular H₂O₂ in cultured endothelial cells, *Arch. Biochem. Biophys.* 302 (2) (1993) 348–355.